HHS Public Access

Author manuscript

Cancer Res. Author manuscript; available in PMC 2017 September 15.

Published in final edited form as:

Cancer Res. 2016 September 15; 76(18): 5442–5454. doi:10.1158/0008-5472.CAN-15-3317.

SMAC mimetic birinapant plus radiation eradicates human head and neck cancers with genomic amplifications of cell death genes *FADD* and *BIRC2*

Danielle F. Eytan[#1,2,3], **Grace E. Snow**[#1,2], **Sophie Carlson**[#1], **Adeeb Derakhshan**[#1,2], **Anthony Saleh**[#1], **Stephen Schiltz**[1], **Hui Cheng**[1], **Suresh Mohan**[1,2], **Shaleeka Cornelius**[1], **Jamie Coupar**[1], **Anastasia L. Sowers**[4], **Lidia Hernandez**[5], **James B. Mitchell**[4], **Christina M. Annunziata**[5], **Zhong Chen**[1,*], and **Carter Van Waes**[1,*]

[1]Tumor Biology Section, Head and Neck Surgery Branch, National Institute on Deafness and Other Communication Disorders, National Institutes of Health, Bethesda, Maryland, USA

[2]NIH Medical Research Scholars Program/HHMI-NIH Scholars Research Program, Cleveland, Ohio, USA

[3]Cleveland Clinic Lerner College of Medicine, Cleveland, Ohio, USA

[4]Radiation Biology Branch, Center for Cancer Research, National Cancer Institute, National Institutes of Health, Bethesda, Maryland, USA

[5]Women's Malignancies Branch, Center for Cancer Research, National Cancer Institute, National Institutes of Health, Bethesda, Maryland, USA

[#] These authors contributed equally to this work.

Abstract

Comparison of tumors from the Cancer Genome Atlas (TCGA) reveals that head and neck squamous cell carcinomas (HNSCC) harbor the most frequent genomic amplifications of *Fas-associated death domain* (*FADD*), with or without Baculovirus Inhibitor of Apoptosis repeat containing BIRC2 (cIAP1), affecting ~30% of patients in association with worse prognosis. Here, we identified HNSCC cell lines harboring *FADD/BIRC2* amplifications and overexpression by exome sequencing, RT-PCR and Western blot. *In vitro*, *FADD* or *BIRC2* siRNA knockdown inhibited HNSCC displaying amplification and increased expression of these genes, supporting their functional importance in promoting proliferation. Birinapant, a novel SMAC mimetic, sensitized multiple HNSCC lines to cell death by agonists TNFα or TRAIL, and inhibited cIAP1>XIAP>IAP2. Combination of birinapant and TNFα induced sub-G0 DNA fragmentation in sensitive lines, and birinapant alone also induced significant G2/M cell cycle arrest and cell death in UM-SCC-46 cells. Gene transfer and expression of *FADD* sensitized resistant UM-SCC-38 cells lacking FADD amplification to birinapant and TNFα, supporting a role for FADD in

[*]**Correspondence:** Carter Van Waes, MD, PhD or Zhong Chen, MD, PhD, National Institute on Deafness and Other Communication Disorders, National Institutes of Health, Building 10/CRC Rm 4-2732 or Rm 5D55, 10 Center Dr., Bethesda, MD 20891. Tel: 301-402-4216; Fax: 301-402-1140; vanwaesc@nidcd.nih.gov or chenz@nidcd.nih.gov.

Disclosure of Potential Conflicts of Interest

Birinapant was provided to NIDCD for research under a Materials Transfer Agreement with the National Cancer Institute and TetraLogic Pharmaceuticals.

sensitization to IAP inhibitor and death ligands. HNSCC varied in mechanisms of cell death, as indicated by reversal by inhibitors or protein markers of caspase-dependent apoptosis and/or RIPK1/MLKL-mediated necroptosis. *In vivo*, birinapant inhibited tumor growth and enhanced radiation induced TNFα, tumor responses, and host survival in UM-SCC-46 and -11B xenograft models displaying amplification and overexpression of *FADD+/−BIRC2*. These findings suggest that combination of SMAC mimetics such as birinapant plus radiation may be particularly active in HNSCC, which harbor frequent *FADD/BIRC2* genomic alterations.

Keywords

birinapant; head and neck cancer; death pathway; xenograft model; radiation

Introduction

Head and neck squamous cell carcinoma (HNSCC) is the sixth most common cancer worldwide, with over 600,000 new cases diagnosed each year, and 5-year survival of ~50% (1). The Cancer Genome Atlas (TCGA) analysis of 279 HNSCC recently uncovered genomic alterations in cell death pathways affecting approximately 40% of HNSCC (2-4). These include ~30% that harbor chromosome 11q13/22 amplifications and overexpression of *Fas-associated death domain* (*FADD*), with or without Baculovirus Inhibitor of Apoptosis repeat containing (*BIRC2/3*) genes that encode cellular Inhibitor of Apoptosis Proteins 1/2 (cIAP1/2). A mutually exclusive subtype (~10%) bears mutations in *caspase-8* (*CASP8*) together with oncogenes *HRAS* or *PIK3CA* (2, 3). Significantly, amplifications of *FADD* without or with *BIRC2* are more often linked to the human papilloma virus-negative [HPV(−)] HNSCCs with worse prognosis (2).

Functionally, FADD, cIAP1/2 and CASP8 are critical components of the Tumor Necrosis Factor (TNF) Receptor family signaling pathways that determine cell death or survival (5-10). Binding of TNFα, TRAIL or other death agonists to their receptors typically leads to cell death via FADD through the activation of caspase-8 and induction of apoptosis, or alternatively, activation of RIP kinase 1 (RIPK1), MLKL, and induction of necroptosis (5-10). However, FADD overexpression has also been implicated in cell growth in lung cancers, and in primary tumors associated with lymph node metastases in HNSCC (11-13), suggesting its function in cancer is context dependent. TNFα-FADD signaling and promotion of cell death via apoptosis or necrosis may be inhibited by cIAPs (14).

IAPs are degraded following binding by the second mitochondria-derived activator of caspases (SMAC), an endogenous protein released by mitochondria at the onset of apoptosis, (15). Targeting IAPs with small molecule mimetics of SMAC can modulate cell death in cancer cells, giving rise to growing interest in their potential as therapeutics (16). Birinapant is a novel bivalent peptidomimetic of SMAC, shown to preferentially target cIAP1, relative to cIAP2 and XIAP (17, 18). Birinapant demonstrated anti-tumor activity in preclinical models of hematological cancers and solid tumors (19,20). In early phase clinical trials, birinapant has demonstrated tolerability and safety at active doses, with a prolonged plasma half-life of 31 hours and tumor half-life of 52 hours (21). In a 5-arm phase I/II dose

escalation study, safety, tolerability and phase II dosing of birinapant in combination with different chemotherapies in patients with solid tumors were established (22). Interestingly, birinapant demonstrated prolonged progression free survival in previously relapsed or refractory patients when combined with chemotherapies known to induce TNFα, such as irinotecan (21, 22). Notably, radiation therapy induces TNFα and cytotoxicity (23, 24), and is a critical modality in treatment of HNSCC.

Here we explore the potential and mechanisms by which HNSCC harboring amplifications and overexpression of *FADD,* without or with *BIRC2,* may be sensitized to SMAC mimetics alone or in combination with TNFα, TRAIL, or radiation.

Materials and Methods

TCGA data analysis

TCGA data was accessed through the cBioPortal for Cancer Genomics (http://www.cbioportal.org/), and queried for FADD, BIRC2, BIRC3, and CASP8 mutation and copy number alterations for all cancer studies (25, 26). Comparison for copy number variation between HPV+ and HPV− used one-sided Wilcoxon signed rank test.

Cell lines and genomic alterations

The eleven HPV(−) and one HPV(+) HNSCC cell lines were authenticated by genotyping using 9 allelic markers (27) and obtained from Dr. T. E. Carey at the University of Michigan (Ann Arbor, MI) in 2010. Stocks were preserved in −80 degrees, cultured as described (27), and used within 3 months.

DNA exome sequencing for copy number and mutations

Genomic DNA was obtained with a DNeasy Blood & Tissue Kit (Qiagen) from frozen cell pellets of UM-SCC lines. Whole exome sequencing with ~87X coverage was performed using SOLiD4 platform (Applied Biosystems, Foster City, CA) and copy number alterations for *FADD* and *BIRC2/3* genes were analyzed using CONTRA and IGA software (28, 29). A *CASP8* mutation was identified using ANNOVAR (http://annovar.openbioinformatics.org/) and Mutation Assessor (http://mutationassessor.org/r3/) using settings specified (Supplementary Methods).

Western blots

UM-SCC cells were plated overnight before treatment with birinapant ± TNFα or TRAIL or 0.01% DMSO diluent control. At 12, 24, and 48 hours after treatment, whole-cell lysates were collected and electrophoresis and western blot was performed, using antibodies, reagents, and conditions specified in Supplementary Methods.

Real-time quantitative polymerase chain reaction

RNA isolation was performed using the RNeasy Mini Kit from Qiagen (Santa Clarita, CA) and on snap frozen tumor samples collected from mice after nine days of treatment using the mirVana miRNA isolation kit from Ambion by Life Technologies (AM1561). The High-capacity cDNA Reverse Transcription Kit (Applied Biosciences, Foster City, CA) was used

per manufacturer's instructions. 30 ng of cDNA was amplified with primers and TaqMan Univeral Master Mix in an ABI Prism 7700 Sequence Detection System (Applied Biosystems, Foster City, CA). Relative gene expression was normalized to 18S control. Samples were assayed in triplicate and presented as the mean +/−s.d. Significance was determined using the student's t-test and *p* values of less than 0.05 were considered statistically significant.

Gene siRNA Knockdown and overexpression

Cells were transfected as described (30) with 50 nM of non-targeting control, BIRC2, BIRC3, and/or FADD siRNA, or 100ng/well empty control pcDNA 3.1 or *FADD* vector plasmids (gifts from Dr. Gabriel Nuñez, University of Michigan) (31), using 0.25 uL/well of Dharmafect Duo (GE Dharmacon, Lafayette, CO) in 100 uL MEM media/well. After 24h, cells were treated with birinapant (10 μM) and/or TNFalpha (20 ng/mL), and viability was assessed via XTT assay 48 and 72 hours following treatment.

XTT and Caspase assays

Cells were plated in 96-well plates and treated with .01% DMSO control or birinapant concentrations indicated ± 20 ng/mL TNFα (R&D systems). Cell density was measured by XTT Kits (Roche) and inhibitory concentration 50% (IC_{50}) was determined at 48-72 hours, as described (Supplementary Methods). To differentiate apoptotic and necroptotic cell death, cells were treated with birinapant ± TNFα, TRAIL, ZVAD, ZIETD or necrostatin (BD Pharmingen). Cells were collected, lysed, and assayed for activity of caspases-3 and -8 using assay kits (Biovision) per manufacturer's protocol on a microplate reader.

DNA Cytofluometry

Cells were plated and treated over 24-72 hours with 0.01% DMSO control, 20 ng/mL TNFα, or 1 μM Birinapant ± TNFα, and prepared for flow cytometry using the Cycle TEST PLUS DNA Reagent Kit (BD Biosciences), for analysis on the FACS Canto flow cytometer (BD Biosciences). Data from 10,000 cells per treatment group and time point were analyzed using BD FACSDiva (BD Biosciences) software.

HNSCC xenograft studies

All animal experiments were carried out under protocol 1322-13 approved by the NIDCD Animal Care and Use Committee. Four- to 6-week-old female SCID/NCr-Balb/c mice and athymic *nu/nu* were obtained from Frederick Cancer Research and Development Center (National Cancer Institute) and housed in a specific pathogen-free animal facility. Mice were injected with UM-SCC cells, randomized, and treated with birinapant and radiation as indicated, and specified in Supplementary Methods.

Immunohistochemistry

Mice harboring UM-SCC-46 tumors were sacrificed after 11 days control and birinapant treatment indicated. Tissue samples were embedded in OCT, and frozen tissue sections were prepared by Histoserv, Inc. (Germantown, MD). Tissue sections were fixed using 4% formalin, permeabilized with methanol, and quenched with 3% H_2O_2. Samples were

blocked using rabbit serum and stained with primary and secondary antibodies specified in Supplementary Methods using the VECTASTAIN Elite ABC Kit (Vector Laboratories, Burlingame, CA). Slides were imaged using the Aperio ScanScope (Leica Biosystems, Buffalo Grove, IL). Histoscores were calculated by ImageScope software (Leica Biosystems).

Statistical design for data analysis

Data from XTT assays and colorimetric assays were presented as mean ± standard deviation. For tumor growth analysis, significance was determined using the student's t-test and p values of less than 0.05 were considered statistically significant. For survival analysis, the Gehan-Breslow-Wilcoxon test was used and significance set to 0.05 using the Bonferroni method.

Results

Frequent genetic alterations of cell death signaling molecules in HNSCC tumors

We surveyed the frequency of gene copy number, mutations, and expression alterations for *FADD, BIRC2, BIRC3* on 11q13/22, and *CASP8* in TCGA datasets, for 279 HNSCC tumor specimens, and other cancers (Figure 1A). Compared with other cancer types, alterations of *FADD* are highest in HNSCC, with ~30% exhibiting amplifications. HNSCC is the second most common tumor with alterations in the *BIRC2/3* locus (8.6%). Alterations of *CASP8*, predominantly mutations, are most frequent in HNSCC (11.2%). Including mRNA up- or downregulation, ~60% of HPV(−) and HPV(+) HNSCC tumors harbor alterations for these genes (Figure 1B). FADD amplification and increased RNA expression is predominantly seen in HPV(−) tumors, and is associated with early recurrence and worse prognosis (Figure 1C, D).

Genetic alterations of cell death signaling molecules in HNSCC cell lines resemble HNSCC tumors

Because of the prevalence and association of *FADD/BIRC2/3* and *CASP8* genomic alterations with HPV(−) HNSCC tumors, we used exome sequencing to examine the genomic alterations of these key cell death pathway components in a panel of 11 human HPV(−) UM-SCC cell lines from patients with poor outcomes (Supplemental Table 1). Consistent with TCGA, focal amplifications of 11q13/22 loci for *FADD* and *BIRC2/3* were found in a subset of UM-SCC lines (Figure 2A). Real-time PCR confirmed an increase in *FADD* mRNA expression of >3-fold in UM-SCC-11A, -11B, -22B, and -46, as compared to primary human oral keratinocytes (HOK) (Figure 2B). *BIRC2* expression was increased >3-fold in UM-SCC-6, -11A, -11B. *BIRC3* was more weakly expressed despite co-amplification. UM-SCC-1 was found to harbor a heterozygous *CASP8* mutation (Q107 nonsense mutation, NS), confirmed recently (3). UM-SCC-11A/B, -22A/B, -38, and -74A/B harbor a common single nucleotide variant resulting in a K14R amino acid change in *CASP8* of unknown functional significance (data not shown). Corresponding FADD, cIAP1, cIAP2 and CASP8 proteins analyzed by Western blot in HOK and UM-SCC cell lines, demonstrated differences in expression largely consistent with the RT-PCR findings (Figure

2C). Thus, differences in genomic alterations and expression of key cell death pathway components in human tumor specimens in TCGA are represented among these cell lines.

Knockdown of *FADD and BIRC2* inhibits growth and sensitizes HNSCC cells to TNF-α

We examined the functional significance of *FADD*, *BIRC2* and *3* by siRNA knockdown alone or with TNF-α in two cell lines differing in amplification and expression of these genes. In UM-SCC-11A, with relatively higher *FADD* and *BIRC2* amplification and expression, *FADD* and *BIRC2* knockdown alone, and in combination with TNFα, decreased cell density as measured by XTT assay (Figure 3A, left; $p<0.001$). In UM-SCC-1 harboring lower amplification and expression of *FADD* and *BIRC2* with the heterozygous *CASP8* Q107 nonsense mutation, weaker inhibition of cell density was observed with knockdown in the absence or presence of TNFα. (Figure 3A, right). The combined effect of *FADD* and *BIRC2* knockdown resulted in similar reduction in cell density as knockdown with either individual gene ($p<0.001$). *BIRC3* knockdown alone had minimal effect, consistent with the low BIRC3 expression. Knockdown of the targets by >80% was confirmed in both lines (Supplemental Figure 1). Together, these data suggest that FADD and BIRC2 overexpression may contribute to growth and/or TNF-α resistance of HNSCC.

Effects of SMAC mimetic birinapant, TNF-α, or TRAIL on cell density, cell cycle, or death in HNSCC cell lines

Since antagonists of BIRCs/IAPs may inhibit cancer cells, we screened the panel of UM-SCC cell lines for sensitivity to SMAC mimetic and IAP inhibitor birinapant by XTT assay over a range of concentrations (1nM-10μM) used in previous studies (20). Figure 3B summarizes the inhibition of cell density of the panel following treatment with birinapant or cell death agonists TNFα or TRAIL alone and in combination, as assessed during exponential growth on day 3, with the IC_{50}s provided in Supplemental Table 2. Multiple cell lines showed enhanced sensitivity to birinapant + TNFα or TRAIL, including many that showed increased expression of FADD and/or other pathway components above. Birinapant alone was most active in UM-SCC-46, with increased expression of FADD, similar BIRC2, but low CASP8 relative to normal HOK cells. An HPV(+) cell line, UM-SCC-47, showed modest sensitivity to birinapant and death ligands. The least TNF-α sensitive cell lines included UM-SCC-9 and 38, displaying weak expression of *FADD/BIRC2*.

We established that gene transfer and overexpression of *FADD*, but not empty vector, enhanced sensitivity of the *FADD*-deficient line UM-SCC-38 to birinapant and TNFα, supporting a distinct function of *FADD* overexpression in sensitization to death ligand when combined with IAP inhibition (Figure 4A). To further evaluate if decreased cell density observed was related to cell cycle and/or cytotoxic effects, DNA cytofluorometric analyses of sensitive UM-SCC-46 and less sensitive UM-SCC-1 cell lines were compared after treatment with birinapant plus TNFα for 48 hours (Figure 4B; Supplemental Figure 2A,B). UM-SCC-46 cells overexpressing FADD treated with birinapant alone, or birinapant and TNFα, exhibited strong increases in sub-G0 DNA indicative of cell death as well as increased G2/M accumulation. By contrast, treatment of UM-SCC-1 cells with weak *FADD* amplification/expression and heterozygous *CASP8* mutation showed a weaker increase in sub-G0 DNA and no accumulation in G2/M following birinapant or combination treatment.

Birinapant plus TNFα induced increased sub-G0 and G2/M DNA in UM-SCC-46 cells in independent experiments (Supplemental Figure 2A, C). UM-SCC-11B expressing both increased FADD and BIRC2, displayed increased sub-G0 DNA but no G2/M DNA accumulation with the combination (Supplemental Figure 2D).

Birinapant sensitizes to TNFα or TRAIL induced cell death through necroptosis and/or apoptosis

To further elucidate the mechanism(s) leading to cell death, we analyzed the effects of pan-caspase (ZVAD), caspase-8 (ZIETD), and RIPK1 (necrostatin) inhibitors on cell density in cell lines with varying cell death pathway alterations (Figure 5A). In UM-SCC-46, RIPK1 inhibition (necrostatin), but not caspase inhibition (ZVAD or ZIETD), reversed the effects of birinapant treatment alone or with death agonists. This data supports predominantly RIPK1-mediated, caspase-independent, necroptotic cell death, consistent with the expression of high FADD, normal BIRC2, and low CASP8 expression observed in UM-SCC-46. Conversely, in UM-SCC-1, the weaker inhibitory effect of birinapant plus death receptor agonists was blocked by both caspase inhibitors ZVAD or ZIETD, but not by necrostatin, supporting predominantly caspase-dependent activity. This cell line exhibits weaker amplification and expression of FADD, and reduced protein expression of BIRC2 and heterozygous wt and mtCASP8. In UM-SCC-74B with normal FADD and BIRC2, but increased expression of a CASP8 sequence variant, pan-caspase inhibitor ZVAD, but not CASP8 inhibitor ZIETD or necrostatin, restored cell density in birinapant plus TNFα or TRAIL treated cells. UM-SCC-11B, which strongly expresses FADD, BIRC2, and CASP8, demonstrated effects by both caspase inhibitors and necrostatin, supporting mixed mechanisms of cell death in this cell line. In UM-SCC-11A, a cell line with high levels of FADD and BIRC2 derived from a biopsy prior to chemotherapy in the same patient, we observed greater sensitivity with a pattern of predominantly caspase-dependent apoptotic cell death. To directly confirm the activation of caspases in UM-SCC-11A, caspase-3 and -8 enzyme assays were used to assess activity with birinapant, TRAIL, or the combination. Birinapant plus TRAIL induced more than a two-fold increase in both caspase-3 and caspase-8 activity in UM-SCC-11A, consistent with the effects observed using the caspase inhibitors.

The expression of key cell death pathway proteins under conditions where treatment with birinapant plus TNFα induced cell death were further examined at different time points in 3 of the lines displaying different patterns of cell death (Figure 5B). Notably, expression of cIAP1, the most sensitive IAP targeted by birinapant, was similarly decreased in all 3 cell lines at 12 hours and remained undetectable up to 48 hours after treatment with birinapant plus TNFα. In the 3 lines, both RIPK1 and RIPK3 showed decreased expression at later time points following drug treatment. UM-SCC-46 demonstrated a greater reduction in FADD and enhancement of necroptosis mediator MLKL expression from 12-48 hours after treatment with birinapant (Figure 5B), consistent with the predominant rescue by necrostatin observed. Interestingly, all 3 lines showed detectable cleavage of caspase-3, although both UM-SCC-1 and -11B showed a relatively greater and sustained increase in CASP3 and CASP8 cleavage, consistent with predominant reversal by both pan- and caspase-8 inhibitors. Although birinapant has been reported to have a lower activity for cIAP2 and XIAP than cIAP1, we performed additional experiments to examine the effects of birinapant

on these IAPs, without and with cIAP1 siRNA knockdown in UM-SCC-46 *in vitro*. Birinapant with control siRNA effectively inhibited cIAP1 partially inhibited XIAP, and weakly enhanced cIAP2 protein expression, whereas BIRC2 siRNA effectively knocked down IAP1 but induced a compensatory increase in cIAP2 that was partially suppressed by combination with birinapant (Supp Fig. 3A). Consistent with this evidence that birinapant also partially inhibits compensatory induction of IAP2, and XIAP, the drug had significantly greater inhibitory effect than that observed with BIRC2/IAP1 knockdown alone, which was weakly attenuated by cIAP1 knockdown alone (Supp Fig. 3B). Together, these data provide evidence that birinapant inhibition of IAPs and death agonists promote cell death via apoptosis and/or necroptosis in HNSCC cell lines with varying alterations affecting cell death components.

Birinapant inhibited tumor growth and prolonged survival in human HNSCC xenograft models with FADD without or with BIRC2 alterations

To evaluate the activity of birinapant *in vivo*, studies were done using UM-SCC-46 (increased FADD expression, normal BIRC2 expression) and UM-SCC-11B (increased FADD and BIRC2 expression) cells in murine xenograft models. SCID mice were implanted with tumor cells, and treated with birinapant, 15 or 30 mg/kg i.p. as reported (20), or control vehicle, when tumors reached 200 mm^3. Birinapant alone versus control had a significant inhibitory effect on tumor growth in both models (Figure 6). For the UM-SCC-46 xenograft model, a significant difference was observed in the mean tumor volumes of the control versus treated animals through day 45 post-tumor cell injection (Figure 6A). Improvement in median survival was observed, from 39 days for control to 58 days in the treated group (Figure 6B). For UM-SCC-11B, prolonged tumor reduction was observed during and after treatment using either 30 mg/kg or 15 mg/kg/day birinapant (Figure 6C). Prolonged host survival was observed in both treatment arms (Figure 5D), with a median of 82 days for control, 137 days for the 30 mg/kg group ($p=0.08$), and >180 days for the 15 mg/kg group ($p=0.05$). The 15 and 30 mg/kg doses of birinapant were well tolerated, and all mice maintained normal body conditioning scores, and weight on treatment (Supplemental Figure 4A,B).

To examine the molecular and cellular effects associated with birinapant treatment *in vivo*, the effects on the IAP cell death pathway components demonstrated above were examined by immunostaining of UM-SCC-46 tumor xenografts during treatment (Day 25) (Figure 6E). In addition, markers of cell death (MLKL, TUNEL) and proliferation (Ki67) were also examined. Tumor immunostaining was quantified by histoscores as described in Methods. Birinapant treatment significantly reduced cIAP1, cIAP2 and XIAP during sustained treatment, supporting contribution of inhibition of these IAPs to the activity *in vivo*. Necroptosis marker MLKL was significantly increased in tumors during the treatment period. There were no significant differences in proliferation (Ki67) or apoptosis (TUNEL) marker staining in tumor specimens at either time point, consistent with the predominantly MLKL/necroptosis-dependent inhibitory effects observed in this model.

Combination of birinapant and radiation induced durable tumor regression and cure in the UM-SCC-46-derived xenograft model

Radiation has previously been shown to induce TNFα (23). We examined the combinatorial effects of birinapant plus radiation *in vivo* using the UM-SCC46 xenograft model, which displayed sensitivity but were not cured by birinapant treatment alone. Tumor cells were injected subcutaneously into the upper leg of athymic *nu/nu* mice, and treated with birinapant(15 mg/kg IP) every 3 days, radiation 2Gy daily M-F for 2 weeks, or the combination when the tumors reached 200 mm^3. Treatment with birinapant or radiation alone significantly delayed tumor growth (Figure 7A) and improved survival (Figure 7B). Remarkably, birinapant combined with radiation cured the animals bearing UM-SCC-46-derived xenografts, with no evidence of disease relapse to 130 days (Figure 7A,B). Representative differences in gross tumor volume amongst treatment arms were observed by day 21, without visual evidence of significant radiation dermatitis, contracture (Figure 7C) or weight loss (Supplemental Figure 3C). As quantified by RT-PCR, TNFα expression in tumors was enhanced by the combination of birinapant plus radiation versus either alone (Figure 7D). To examine if radiosensitization by birinapant observed is due to intrinsic or TNFα-enhanced radiosensitivity of UMSCC-46, cells were treated with 30 nM birinapant immediately after radiation, and re-plated after 24 hours for clonogenic assay. Interestingly, in vitro combination of birinapant alone with radiation over a range of 0-9Gy had no significant direct radiosensitizing effect over that due to radiation alone (Supp Fig 5A), suggesting that the activity observed *in vivo* is dependent on additional factor(s). As we hypothesized and observed that birinapant plus radiation potently induces endogenous TNFα in tumors in vivo (Fig 7D), we examined and confirmed that combination of TNFα (2ng/ml) with birinapant significantly enhances radiation sensitivity at 3Gy compared to the single agents (Supp Fig 5B). Combination birinapant and radiation or radiation alone also significantly suppressed tumor growth in FADD- and BIRC2-overexpressing UM-SCC-11B xenografts, but not UM-SCC-1 xenografts displaying weaker *FADD/BIRC2* copy gain and expression, and a heterozygous *CASP8* mutation (Supplemental Figure 6). Together, these findings support birinapant plus radiation as a therapeutic combination for HNSCC harboring genomic amplification or increased expression of FADD without or with BIRC2.

Discussion

TCGA linked amplification of 11q13 containing *FADD* with a major subset of HPV(−) HNSCC (2). 11q22 harboring *BIRC2/3* encoding IAP1/2 was often co-amplified. *CASP8* was mutated in a mutually exclusive subset. These molecules comprise core components of the TNF receptor family signal pathways that regulate the balance between cell death via apoptosis and necroptosis, or cell survival (Figure 7E). SMAC mimetics promote degradation of IAP proteins that inhibit the intrinsic and extrinsic cell death signaling pathways, potentially overcoming resistance to death ligands and radiation (16, 32). Here, we present evidence that HNSCC with genomic alterations in these cell death pathway components are sensitive to combinations of a SMAC mimetic plus death ligands TNFα, TRAIL or radiation.

Our TCGA analysis indicates that *FADD* amplification is more frequent in HNSCC than other cancers, and is associated with early recurrence and worse prognosis. We observed increase in gene copy number and expression of *FADD* with or without *BIRC2*, while *BIRC3* was minimally expressed, among a subset of human HPV(−) HNSCC cell lines, consistent with HNSCC tumors (2). A heterozygous mutation of *CASP8* was detected in only 1/11 cell lines, approximating the frequency in tumors. Knockdown of *FADD* or *BIRC2*, but not *BIRC3*, inhibited and enhanced TNF-α sensitivity of UM-SCC-11A cells harboring amplification and increased expression of *FADD* and *BIRC2*, which have been implicated in promoting cell proliferation, and resistance to TNFα induced cell death (11-14).

Multiple HNSCC lines overexpressing one or more of these cell death pathway components exhibited pharmacologic inhibition by the SMAC mimetic birinapant in combination with TNFα or TRAIL. This inhibition accompanied a corresponding increase in cell death, supported by increased sub-G0 DNA fragmentation, and reversibility by caspase and/or RIPK1/3 inhibitor(s). Birinapant plus TNFα promoted degradation of cIAP1, the product of *BIRC2*, and variably activated caspase and/or MLKL mediators of apoptosis or necroptosis in different HNSCC. These findings implicate IAPs as critical mediators of the widespread resistance of HNSCC to TNFα previously observed by our laboratory (33). Birinapant activity was also associated with reproducible effects on G2/M cell cycle progression in UM-SCC-46 cells, similar to that reported with natural IAP inhibitor embelin in PC3 prostate cancer cells (32), and recently linked to the role of FADD in proliferation in lung carcinoma (34). In the latter study, the induction of mitosis and lung carcinogenesis depended upon activation of KRAS, and CK1α phosphorylation of FADD during G2/M, where FADD interacted with G2/M cell cycle regulatory components PLK1, AURKA and BUB1. Interestingly, UM-SCC-46 showed a greater reduction in FADD by birinapant and TNFα during 48 hours post treatment when G2/M arrest was observed, compared with other lines lacking this effect. However, after sustained monotherapy *in vivo*, resumption of tumor growth was observed, and we detected no difference in Ki-67 staining. Whether there is sustained G2/M block, or compensatory mechanism(s) of proliferation with prolonged treatment *in vivo*, merits further investigation. Of potentially broader clinical relevance, birinapant combined with cell death ligands was capable of inducing potent cytotoxicity in HNSCC lines that were derived from aggressive primary, metastatic, and recurrent tumors, that are often mutant or deficient for pro-death tumor suppressor *TP53* (2).

We observed differences in sensitivity to death ligands and predominant cell death pathways and mechanisms upon comparison of HNSCC harboring different alterations in *FADD*, *BIRC2* and *CASP8*. Evidence for caspase–dependent apoptosis, RIPK/MLKL-dependent necroptosis, or mixed mechanisms of cell death were observed by comparing the effects of reversible inhibitors and established markers of caspase and/or RIPK-dependent pathways. Birinapant and TNF α-mediated cytotoxicity of UM-SCC-11B with *FADD/BIRC2* amplification and normal *CASP8* expression was reversed by pan-caspase and CASP8 inhibitors, and showed increased caspase-3 or -8 cleavage, supporting predominantly caspase-dependent mechanisms of apoptosis. By contrast, inhibition of UM-SCC-46 was predominantly reversed by the RIPK1 inhibitor necrostatin and associated with induction of MLKL *in vitro* and *in vivo*, supporting necroptosome-dependent inhibition in this HNSCC

overexpressing FADD but low caspase-8 protein. Since caspase-8 has been shown to inhibit necrosis while promoting apoptosis (35), low CASP8 expression could explain the predominantly necroptotic cell death seen in UM-SCC46. Interestingly, UM-SCC-74B, expressing a common K14R amino acid variant of CASP8, and lower FADD and BIRC2, demonstrated sensitivity to birinapant and death ligands reversible by pan-caspase but not caspase-8 inhibitors, consistent with caspase-8 independent cell death mechanisms. Further experiments provided evidence birinapant can also partially inhibit XIAP expression, which could potentially enhance other caspase-dependent mechanisms. Compared to these lines, UM-SCC-1 with lower amplification and expression of *FADD/BIRC2* and a heterozygous *CASP8* mutation was relatively less sensitive *in vitro* and *in vivo*. Inhibition of UM-SCC-1 and 11B was reversed by both caspase and necroptosis inhibitors and demonstrated cleaved caspase and basal MLKL expression, supporting mixed mechanisms. Raulf *et al*. found evidence for mixed apoptotic and necroptotic cell death in response to a SMAC mimetic in HNSCC cell line HSC3, and not others, but the genomic alterations were undefined (36). Together, these observations suggest that the status of *FADD, BIRC2*, *CASP8* and other components of the cell death machinery may affect sensitivity to these agents, and merit further investigation as potential predictive biomarkers for response in future clinical studies of SMAC mimetics in HNSCC.

Our *in vivo* preclinical studies demonstrate that two independent models with genomic alterations in FADD−/+BIRC2 amplification exhibited significant sensitivity and prolonged survival following birinapant treatment alone, despite differences in intrinsic sensitivity *in vitro*. Birinapant alone induced endogenous TNFα mRNA *in vivo*, but the incomplete suppression of tumor growth with birinapant monotherapy suggested that this level alone may be insufficient to potentiate tumor regression. Birinapant plus radiation led to more durable responses in UM-SCC-46 and 11B xenograft models. Further, the combination of birinapant plus radiation more potently enhanced the expression of endogenous murine TNFα compared to either therapy alone. While birinapant alone did not significantly enhance the effects of radiation *in vitro*, addition of TNFα enhanced radiosensitization in clonogenic assay. Because TNFα is induced in tumors following radiation treatment (23), studying the addition of birinapant plus radiation holds considerable clinical relevance to this standard treatment for HNSCC.

Recently, combinatorial activity of different SMAC mimetics with radiation and induction of TNFα has been demonstrated in lung cancer and HNSCC cell lines (37,38). Partial response in UM-SCC-1 xenografts in the latter study was observed, similar to our results. The relative contribution of weaker amplification of FADD/BIRC2 and/or heterozygous mutation of CASP8 to the resistance to birinapant plus TNFα or radiation in this model may merit future investigation. Together, these observations underscore the importance of assessing genomic alterations, expression, and the molecular and antitumor effects of targeting cell death pathways with SMAC mimetics in preclinical studies and future clinical trials in HNSCC and other cancers. FADD/BIRC2 alterations may represent an Achilles' heel for his subset of HNSCC, and for clinical investigation with SMAC mimetics.

Supplementary Material

Refer to Web version on PubMed Central for supplementary material.

Acknowledgements

This study utilized the high-performance computational capabilities of the Biowulf Linux cluster at the National Institutes of Health, Bethesda, MD (http://biowulf.nih.gov). Thanks to Barbara Conley and James F. Battey for reading and helpful comments on the manuscript.

Grant Support: NIDCD intramural projects ZIA-DC-000016, 73, 74 (C. Van Waes, A. Saleh, S. Schiltz, H. Cheng, S. Cornelius, J. Coupar) and the NIH-Medical Research Scholars Program (D.F. Eytan, G.E. Snow, S. Mohan, A. Derahkshan).

References

1. Siegel R, Naishadham D, Jemal A. Cancer statistics, 2013. CA Cancer J Clin. 2013; 63:11–30. [PubMed: 23335087]
2. The Cancer Genome Atlas Network. Comprehensive genomic characterization of head and neck squamous cell carcinomas. Nature. 2015; 517:576–82. [PubMed: 25631445]
3. Pickering CR, Zhang J, Yoo SY, Bengtsson L, Moorthy S, Neskey DM, et al. Integrative genomic characterization of oral squamous cell carcinoma identifies frequent somatic drivers. Cancer Discov. 2013; 3:770–81. [PubMed: 23619168]
4. Stransky N, Egloff AM, Tward AD, Kostic AD, Cibulskis K, Sivachenko A, et al. The mutational landscape of head and neck squamous cell carcinoma. Science. 2011; 333:1157–60. [PubMed: 21798893]
5. Festjens N, Vanden Berghe T, Cornelis S, Vandenabeele P. RIP1, a kinase on the crossroads of a cell's decision to live or die. Cell Death Differ. 2007; 14:400–10. [PubMed: 17301840]
6. Gyrd-Hansen M, Meier P. IAPs: from caspase inhibitors to modulators of NF-kappaB, inflammation and cancer. Nature Rev Cancer. 2010; 10:561–74. [PubMed: 20651737]
7. Moquin DM, McQuade T, Chan FK. CYLD deubiquitinates RIP1 in the TNFalpha-induced necrosome to facilitate kinase activation and programmed necrosis. PloS One. 2013; 8:e76841. [PubMed: 24098568]
8. Oberst A, Dillon CP, Weinlich R, McCormick LL, Fitzgerald P, Pop C, et al. Catalytic activity of the caspase-8-FLIP(L) complex inhibits RIPK3-dependent necrosis. Nature. 2011; 471:363–7. [PubMed: 21368763]
9. Oberst A, Green DR. It cuts both ways: reconciling the dual roles of caspase 8 in cell death and survival. Nature Rev Mol Cell Biol. 2011; 12:757–63. [PubMed: 22016059]
10. Varfolomeev E, Blankenship JW, Wayson SM, Fedorova AV, Kayagaki N, Garg P, et al. IAP antagonists induce autoubiquitination of c-IAPs, NF-kappaB activation, and TNFalpha-dependent apoptosis. Cell. 2007; 131:669–81. [PubMed: 18022362]
11. Bhojani MS, Chen G, Ross BD, Beer DG, Rehemtulla A. Nuclear localized phosphorylated FADD induces cell proliferation and is associated with aggressive lung cancer. Cell cycle. 2005; 4:1478–81. [PubMed: 16258269]
12. Chen G, Bhojani MS, Heaford AC, Chang DC, Laxman B, Thomas DG, et al. Phosphorylated FADD induces NF-kappaB, perturbs cell cycle, and is associated with poor outcome in lung adenocarcinomas. Proc Nat Acad Sci USA. 2005; 102:12507–12. [PubMed: 16109772]
13. Pattje WJ, Melchers LJ, Slagter-Menkema L, Mastik MF, Schrijvers ML, Gibcus JH, et al. FADD expression is associated with regional and distant metastasis in squamous cell carcinoma of the head and neck. Histopathology. 2013; 63:263–70. [PubMed: 23763459]
14. Wang CY, Mayo MW, Korneluk RG, Goeddel DV, Baldwin AS Jr. NF-kappaB antiapoptosis: induction of TRAF1 and TRAF2 and c-IAP1 and c-IAP2 to suppress caspase-8 activation. Science. 1998; 281:1680–3. [PubMed: 9733516]

15. Long JS, Ryan KM. New frontiers in promoting tumour cell death: targeting apoptosis, necroptosis and autophagy. Oncogene. 2012; 31:5045–60. [PubMed: 22310284]
16. Fulda S, Vucic D. Targeting IAP proteins for therapeutic intervention in cancer. Nature Rev Drug Discov. 2012; 11:109–24. [PubMed: 22293567]
17. Condon SM, Mitsuuchi Y, Deng Y, LaPorte MG, Rippin SR, Haimowitz T, et al. Birinapant, a smac-mimetic with improved tolerability for the treatment of solid tumors and hematological malignancies. J Med Chem. 2014; 57:3666–77. [PubMed: 24684347]
18. Mitsuuchi Y, Condon SM, Neiman EM, Benetatos CA, Seipel ME, Kapoor GS, et al. Birinapant, a novel bivalent SMAC mimetic drug, is superior to monovalent SMAC mimetics in inhibition of NF-κB by targeting TRAF-2 bound cIAP1 and cIAP2. Amer Assoc Cancer Res Proceedings. 2013:3333.
19. Allensworth JL, Sauer SJ, Lyerly HK, Morse MA, Devi GR. Smac mimetic Birinapant induces apoptosis and enhances TRAIL potency in inflammatory breast cancer cells in an IAP-dependent and TNF-alpha-independent mechanism. Breast Cancer Res Treat. 2013; 137:359–71. [PubMed: 23225169]
20. Benetatos CA, Mitsuuchi Y, Burns JM, Neiman EM, Condon SM, Yu G, et al. Birinapant (TL32711), a bivalent SMAC mimetic, targets TRAF2-associated cIAPs, abrogates TNF-induced NF-kappaB activation, and is active in patient-derived xenograft models. Mol Cancer Ther. 2014; 13:867–79. [PubMed: 24563541]
21. Senzer NN, LoRusso P, Martin LP, Schilder RJ, Amaravadi RK, Papadopoulos KP, et al. Phase II clinical activity and tolerability of the SMAC-mimetic birinapant (TL32711) plus irinotecan in irinotecan-relapsed/refractory metastatic colorectal cancer. J Clin Oncol. 2013; (suppl) abstr 3621.
22. Amaravadi RK, Senzer NN, Martin P, Schilder RJ, LoRusso P, Papadopoulos KP, et al. A phase I study of birinapant (TL32711) combined with multiple chemotherapies evaluating tolerability and clinical activity for solid tumor patients. J Clin Oncol. 2013; (suppl) abstr 2504.
23. Hallahan DE, Spriggs DR, Beckett MA, Kufe DW, Weichselbaum RR. Increased tumor necrosis factor alpha mRNA after cellular exposure to ionizing radiation. Proc Nat Acad Sci USA. 1989; 86:10104–7. [PubMed: 2602359]
24. Xanthinaki A, Nicolatou-Galitis O, Athanassiadou P, Gonidi M, Kouloulias V, Sotiropoulou-Lontou A, et al. Apoptotic and inflammation markers in oral mucositis in head and neck cancer patients receiving radiotherapy: preliminary report. Supp Care Cancer. 2008; 16:1025–33.
25. Cerami E, Gao J, Dogrusoz U, Gross BE, Sumer SO, Aksoy BA, et al. The cBio cancer genomics portal: an open platform for exploring multidimensional cancer genomics data. Cancer Discov. 2012; 2:401–4. [PubMed: 22588877]
26. Gao J, Aksoy BA, Dogrusoz U, Dresdner G, Gross B, Sumer SO, et al. Integrative analysis of complex cancer genomics and clinical profiles using the cBioPortal. Science Signal. 2013; 6:pl1.
27. Brenner JC, Graham MP, Kumar B, Saunders LM, Kupfer R, Lyons RH, et al. Genotyping of 73 UM-SCC head and neck squamous cell carcinoma cell lines. Head Neck. 2010; 32:417–26. [PubMed: 19760794]
28. Li J, Lupat R, Amarasinghe KC, Thompson ER, Doyle MA, Ryland GL, et al. CONTRA: copy number analysis for targeted resequencing. Bioinformatics. 2012; 28:1307–13. [PubMed: 22474122]
29. Robinson JT, Thorvaldsdottir H, Winckler W, Guttman M, Lander ES, Getz G, et al. Integrative genomics viewer. Nature Biotech. 2011; 29:24–6.
30. Yang X, Lu H, Yan B, Romano RA, Bian Y, Friedman J, et al. DeltaNp63 versatilely regulates a Broad NF-kappaB gene program and promotes squamous epithelial proliferation, migration, and inflammation. Cancer Res. 2011; 71:3688–700. [PubMed: 21576089]
31. Inohara N, Koseki T, Hu Y, Chen S, Núñez G. CLARP, a death effector domain-containing protein interacts with caspase-8 and regulates apoptosis. Proc Natl Acad Sci U S A. 1997; 94:10717–22. [PubMed: 9380701]
32. Dai Y, Desano J, Qu Y, Tang W, Meng Y, Lawrence TS, et al. Natural IAP inhibitor Embelin enhances therapeutic efficacy of ionizing radiation in prostate cancer. Amer J Cancer Res. 2011; 1:128–43. [PubMed: 21804946]

33. Duffey DC, Crowl-Bancroft CV, Chen Z, Ondrey FG, Nejad-Sattari M, Dong G, et al. Inhibition of transcription factor nuclear factor-kappaB by a mutant inhibitor-kappaBalpha attenuates resistance of human head and neck squamous cell carcinoma to TNF-alpha caspase-mediated cell death. Br J Cancer. 2000; 83:1367–74. [PubMed: 11044363]

34. Bowman BM, Sebolt KA, Hoff BA, Boes JL, Daniels DL, Heist KA, et al. Phosphorylation of FADD by the kinase CK1α promotes KRASG12D-induced lung cancer. Sci Signal. 2015; 8:ra9. [PubMed: 25628462]

35. O'Donnell MA, Perez-Jimenez E, Oberst A, Ng A, Massoumi R, Xavier R, et al. Caspase 8 inhibits programmed necrosis by processing CYLD. Nat Cell Biol. 2011; 13:1437–42. [PubMed: 22037414]

36. Raulf N, El-Attar R, Kulms D, Lecis D, Delia D, Walczak H, et al. Differential response of head and neck cancer cell lines to TRAIL or Smac mimetics is associated with the cellular levels and activity of caspase-8 and caspase-10. Br J Cancer. 2014; 111:1955–64. [PubMed: 25314064]

37. Liu N, Tao Z, Blanc JM, Zaorsky NG, Sun Y, Vuagniaux G, et al. Debio 1143, an antagonist of multiple inhibitor-of-apoptosis proteins, activates apoptosis and enhances radiosensitization of non-small cell lung cancer cells in vitro. Amer J Cancer Res. 2014; 4:943–51. [PubMed: 25520882]

38. Yang J, McEachern D, Li W, Davis MA, Li H, Morgan MA, et al. Radiosensitization of head and neck squamous cell carcinoma by a SMAC-mimetic compound, SM-164, requires activation of caspases. Molecular Cancer Ther. 2011; 10:658–69.

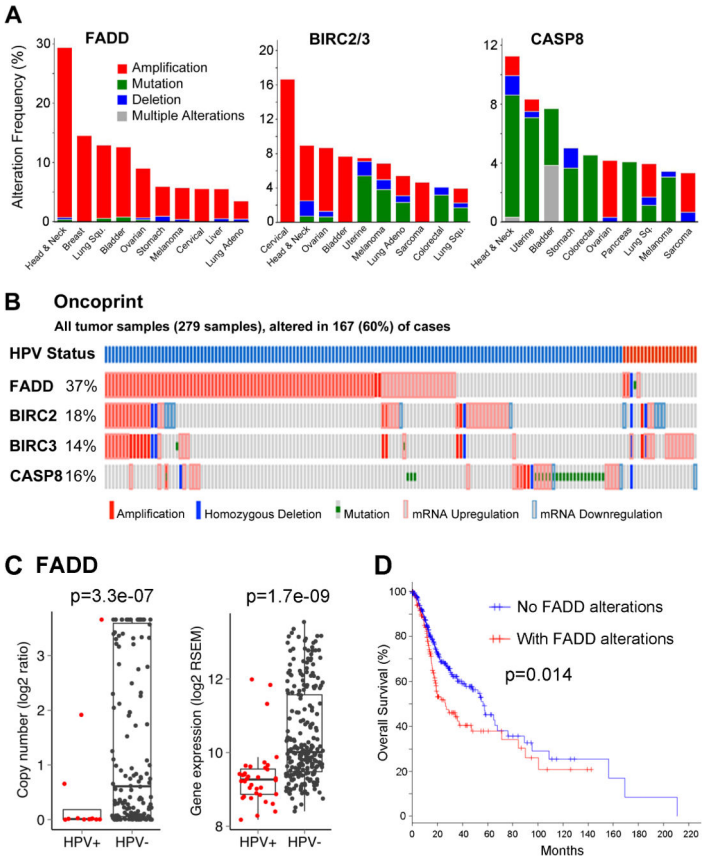

Figure 1.

Genetic alterations of cell death pathway components in HNSCC and other cancer types from TCGA datasets. **A**, Genetic alterations of FADD, BIRC2, BIRC3, and CASP8 for top ten tumor types. DNA amplification (red), mutation (green), and deletion (blue), or multiple defects (grey). **B**, Oncoprint showing genetic and expression alterations from 279 HNSCC samples. Vertical bars represent alterations for single specimens. Top bars, blue HPV(−), red HPV(+). **C**, Scatter plots, FADD amplification and overexpression is predominantly associated with HPV(−) tumors. P values are comparing HPV+ and HPV− with one-sided Wilcoxon signed rank test. **D**, Kaplan-Meier survival plots for FADD in 279 HNSCC in TCGA.

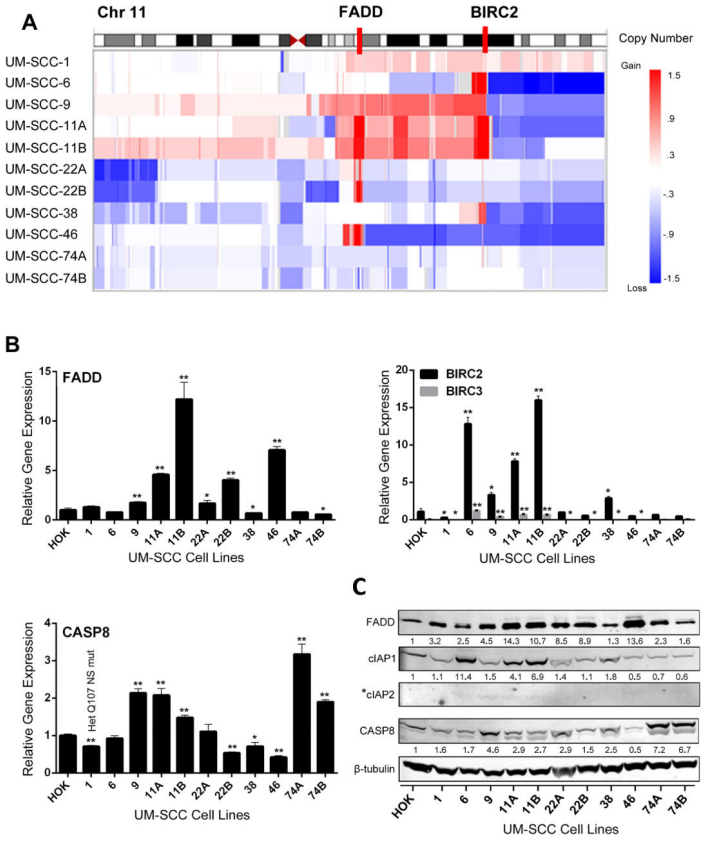

Figure 2.

Copy variation and expression of FADD, BIRC2/3 and CASP8 by HNSCC lines. **A**, Chromosome 11q13/11q22 FADD/BIRC2 loci (red bars) copy variation in UM-SCC lines. Heat maps show segmented copy number variations; red, gain; blue, loss; and white, no change. **B**, qRT-PCR data showing relative fold expression of FADD, BIRC2, BIRC3, and CASP8 in UM-SCC cell lines normalized to expression levels in primary human oral keratinocytes (HOK). UM-SCC-1 harboring a *CASP8* heterozygous Q107 nonsense mutant is indicated. *p<0.05; **p<0.001 versus HOK, Student t-test. **C**, Western blot of proteins from whole cell lysates of HOK and UM-SCC cell lines. Expression was quantified by densitometry comparison to HOK and β-tubulin as a loading control, except where *IAP2 is undetectable in HOK.

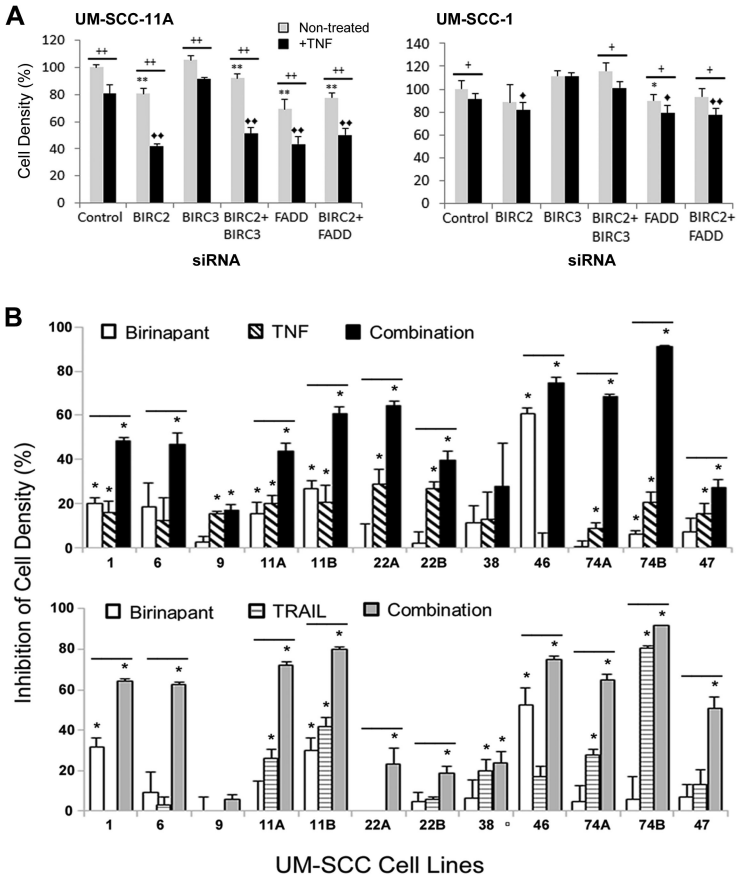

Figure 3.

Effects of BIRC2 and FADD siRNA knockdown or birinapant, TNFα, and TRAIL on UM-SCC cell lines. **A,** Cell density UM-SCC-11A and UM-SCC-1 measured by XTT at 3 days post treatment after control, BIRC2, BIRC3, and/or FADD siRNA knockdown, −/+20 ng/mL TNFα. Cell density, as percent of control siRNA, no TNFα. Error bars, standard deviation of 3 replicates. Student t-test: * $p<0.05$, **$p<0.001$ vs control siRNA; <>$p<0.05$, <><>$p<0.001$ vs control siRNA+TNFα; + $p<0.05$, ++ $p<0.001$ TNFα versus no TNFα. **B**, Percent growth inhibition by XTT assays on day 3 post treatment in UM-SCC cell panel treated with 1 μM birinapant, 20 ng/mL TNFα (top), 50 ng/mL TRAIL (bottom), or the combinations. Non-treated and birinapant controls for comparison with TNFα or TRAIL or their combinations were performed in independent experiments. Values normalized to non-treated cells for the same experiment, $p<0.05$, *, compared with control; bar, combination vs birinapant alone, Student t-test.

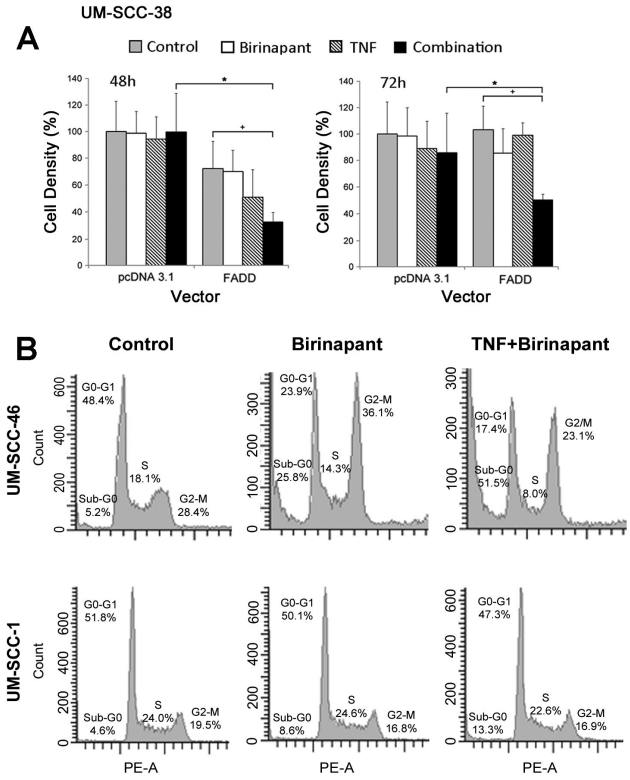

Figure 4.

Effect of brinapant and TNFα on cell proliferation in FADD-deficient UM-SCC-38 following overexpression of FADD vector, and on cell cycle DNA in UM-SCC-46 and 1 with greater and weaker FADD expression. **A**, Cellular proliferation in UM-SCC-38 following transfection with pcDNA 3.1 or FADD vector by XTT at 48 and 72hours post treatment with 10 μM birinapant and/or 20 ng/mL TNFα. Student t-test, * $p<0.05$ for empty vector vs. FADD; + $p<0.05$ comparing FADD control vs. FADD plus combination. **B,** UM-SCC-46 and -1 cells were treated with 1 μM birinapant with or without 20 ng/mL TNFα, and harvested at 48 hours post-treatment for DNA cell cycle cytofluorometry. Histograms with % cells with sub-G0, G0/G1, S and G2/M DNA.

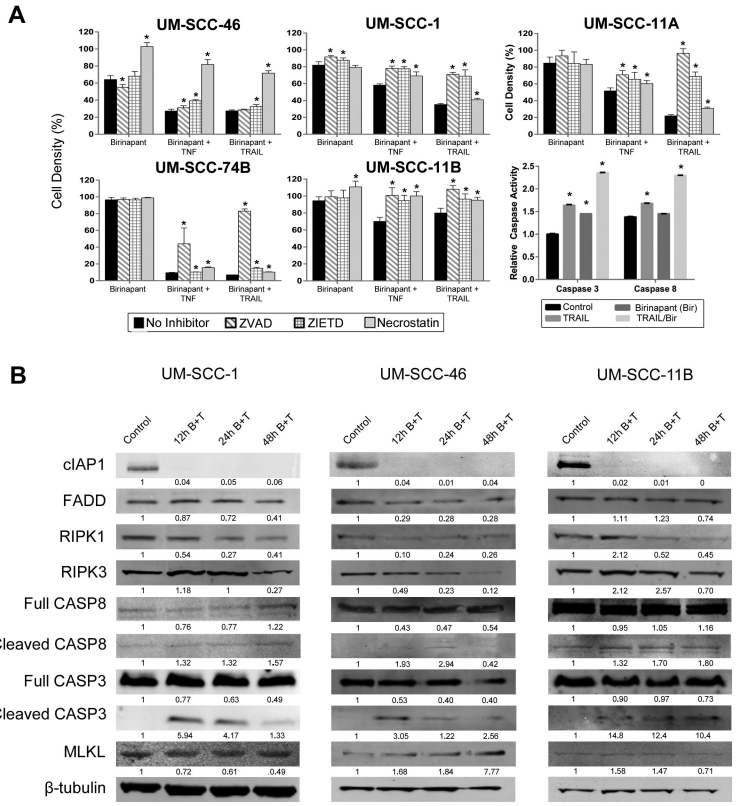

Figure 5.

Birinapant plus death ligands induced cell death in UM-SCC lines via caspase and/or necroptosis dependent mechanisms. **A**, Cell lines were treated with combinations of 1 μM birinapant, 20 ng/mL TNFα, 50 ng/mL TRAIL, 20 μM ZVAD (pan-caspase inhibitor), 20 μM ZIETD (caspase-8 inhibitor), or 20 μM necrostatin-1 (RIPK1 inhibitor) and assessed for effect on cell density or caspase-3 and -8 activation. Standard error bars for 3 replicates, Student t-test, *p<0.05. **B,** In independent experiments, UM-SCC-1, -46, and -11B cell lines were treated with 0.01% DMSO diluent control, or 1 μM birinapant and 20 ng/mL TNFα (B+T), and whole cell lysates procured 12, 24, and 48 hours after treatment were subjected to SDS-PAGE and Western blots. Expression for each protein was quantified and normalized to both diluent control (=1) and β-tubulin loading control for the respective lane for the blots shown for each cell line.

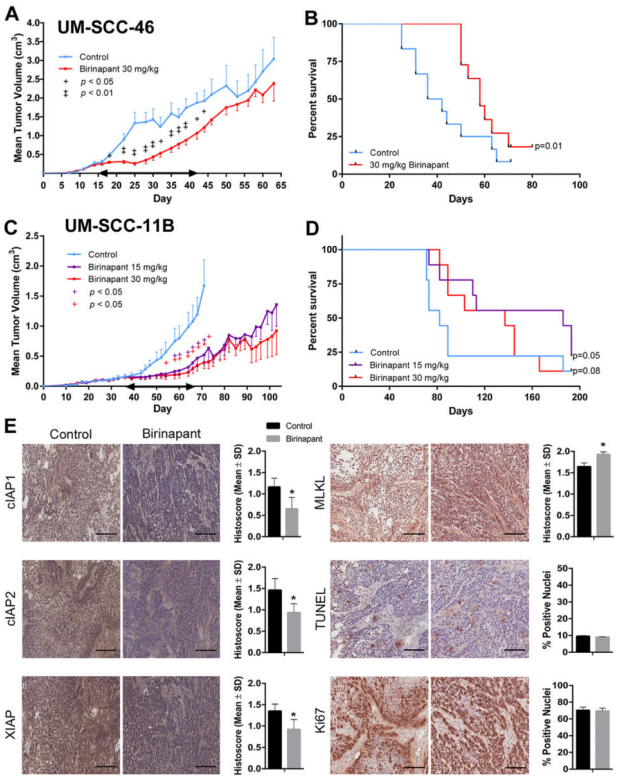

Figure 6.

Birinapant effects on tumor growth, survival, and molecular markers in human HNSCC xenograft models. 5×10^6 UM-SCC-46 FADD or -11B FADD and BIRC2 amplified cells were injected subcutaneously into SCID/NCr-Balb mice. Mice were randomized (UM-SCC-46 n=15 mice/group; UM-SCC-11B n=9 mice/group) and treatment was initiated day 15 and 35 after tumor inoculation, when tumors reached 200 mm^3. Control vehicle, 15 or 30 mg/kg birinapant i.p. was given every 3 days × 10 doses (double-ended arrow). **A, B**, UM-SCC46, birinapant treatment significantly inhibited tumor volume versus control vehicle (+, $p<0.05$; ++, $p<0.01$), and improved median survival (58 versus 39 days). **C, D,** UM-SCC-11B, birinapant-treatment significantly inhibited tumor volume versus control vehicle (+, $p<0.05$; ++, $p<0.01$), and increased median survival (Gehan-Breslow-Wilcoxon test and the Bonferroni method, $p<0.05$). **E,** *In vivo* effects of birinapant treatment on cIAP1, cIAP2, XIAP, TUNEL and Ki67 proliferation markers in UM-SCC-46 xenograft mouse model of HNSCC. Photomicrographs show immunostaining done on frozen sections of tumors harvested on treatment (Day 25). Bar: 200 μM. Staining histoscores for untreated (black) and birinapant-treated mice (gray). Student t-test (*, $p<0.01$).

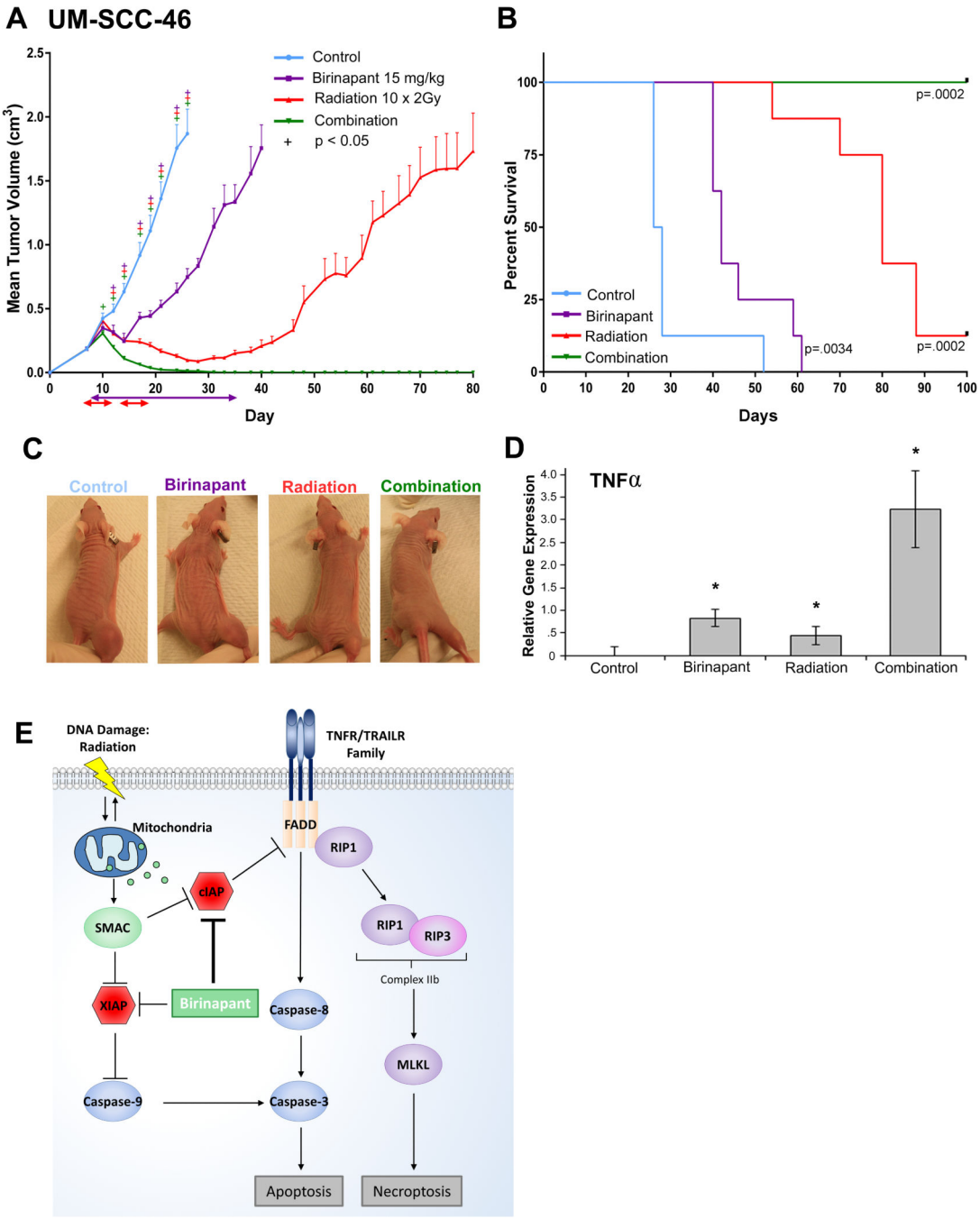

Figure 7.

Birinapant plus radiation induces tumor regression in xenografts, and model of cell death pathways modulated by birinapant. **A,** 2.5×10^6 UM-SCC-46 cells were implanted into athymic *nu/nu* mice. Mice were randomized into four groups (vehicle control, 15 mg/kg birinapant, 10 × 2 Gy radiation, or combination, n=12 each) seven days after tumor inoculation (day 7) when average tumor volume reached ~200 mm^3. Radiation beginning day 7: 2 Gy of radiation given M-F for two weeks, to 20 Gy (red double headed arrows). Birinapant beginning day 8: 15 mg/kg birinapant i.p. every three days for ten doses (purple

double headed arrow). Statistical difference vs control by Student t-test (+; $p < 0.05$). Error bars, SEM. **B,** Survival analysis, significance determined by Gehan-Breslow-Wilcoxon test. Median survival, 27 days (control), 42 days (birinapant, p=0.003), 80 days (radiation, p=0.0002), and combination group without deaths, to 100 days. **C**, Photos of tumors of representative mice from each treatment group on day 21 (five doses of birinapant and 20 Gy radiation). **D**, Relative mTNFα gene expression in tumors on day 21 compared by qRT-PCR. Student t-test (*; $p < 0.05$). Error bars, SEM. **E**, The intrinsic cell death pathway, inducible by radiation DNA damage, and the extrinsic pathway, triggered by death receptor family ligands can converge on caspase-3 to induce apoptosis. Death ligand binding via the extrinsic pathway results in a cytoplasmic complex that includes FADD, which may activate caspase-8/3, or RIP1/3/MLKL-mediated signaling and necroptosis. Cell death is blocked by Inhibitors of Apoptosis Proteins (IAPs). DNA damage induced mitochondrial release of SMAC, and SMAC mimetic birinapant inhibits and degrades IAPs (cIAP1, cIAP2, XIAP) to enhance TNF-mediated cell death.